

Study on Target Residues from the Interaction of Copper with 44 MeV/A ^{12}C Ions

Li Wenxin, Sun Tongyu, Sun Rulin, Wu Dingqing, Zhao Lili and Jing Genming

Institute of Modern Physics, Chinese Academy of Sciences, Lanzhou, Gansu, China

Qi Dahai and Sa Benhao

Institute of Atomic Energy, Beijing, China

Cross sections and average forward ranges were determined for 35 target residues from the interaction of copper with 44 MeV/A ^{12}C ions by nuclear chemistry techniques. From these data the isobaric yield distribution, the mass yield distribution and the longitudinal momentum transfer were obtained. The mass yield distribution and the isobaric yield distribution are in good agreement with those calculated from a modified statistical model and corresponding Monte Carlo technique.

1. INTRODUCTION

In recent years, the study of intermediate energy heavy-ion reactions has attracted considerable interest because the change in the dynamics of the interaction would be expected to occur in this energy region. It is well known that low-energy ($E_i \leq 10$ MeV/A) reactions are dominated by mean field dynamics and involve complete fusion and deep inelastic processes. On the other hand, high-energy ($E_i \geq 200$ MeV/A) reactions involve the dynamics of nucleon-nucleon collision, and can be explained by the participant-spectator model. While both the low- and high-energy regimes have been studied for many years, the regime of intermediate energy has become a attractive research subject only in recent years, with the advent of intermediate energy heavy ion accelerators.

As a first set of experiments performed on the Heavy Ion Research Facility (HIRFL) at Institute of Modern Physics, Lanzhou, we have studied the interactions of Cu, ^{93}Nb and ^{181}Ta with ~ 47 MeV/A ^{12}C ions by use of radiochemical techniques combined with the thick target-thick

foil method. In this paper we report the results of a study of the yields and the mean longitudinal momentum transfer of the target residues from the reaction of natural copper with 44 MeV/A ^{12}C ions.

The cross sections and thick target recoil properties of the products have been reported for the interaction of natural copper with 86 MeV/A ^{12}C ions [1-3]. Cho and his coworkers have studied the mass distribution and the longitudinal momentum transfer in the reaction of Cu with 35 MeV/A ^{12}C [4]. Recently they extended a similar study to the region of 15-45 MeV/A ^{12}C ions [5]. Pienkowski *et al.*, however, have studied 10-50 MeV/A $^{20}\text{Ne} + \text{Cu}$ reactions with thick target-thick catcher foils [6].

Theoretical explanation for the experimental data in the intermediate energy reactions is not always successful. So far as the mass yield distribution of the target fragments, neither cascade evaporation calculation [2] with Monte Carlo technique nor the evaporation code EVA and the preequilibrium code ALICE [4] describing the deexcitation processes on the assumption of incomplete fusion could satisfactorily agree with the mass distributions for the reactions of Cu with 86 MeV/A and 35 MeV/A ^{12}C ions. Using a statistical multifragmentation model, however, Sa Benhao *et al.* successfully reproduced the mass distribution of 35 MeV/A $^{12}\text{C} + \text{Cu}$ reaction [7]. This work was taken with the purpose of measuring the mass distribution for 44 MeV/A $^{12}\text{C} + \text{Cu}$ reaction and, by comparison with the statistical multifragmentation model, of examining the validity of the theory. Furthermore the mean longitudinal momentum transfer associated with the formation of specific products was measured in order to gain more information on the evolution of the reaction mechanisms.

2. EXPERIMENT

The irradiation was performed on HIRFL at the Institute of Modern Physics, Chinese Academy of Sciences. The target assembly was a 99.99% pure copper foil, 18.0 mg/cm² thick, surrounded by two Mylar foils. The Cu target assembly and a Nb target assembly formed in a similar manner were irradiated simultaneously. Additional Mylar foils serving as activation blanks were placed on each side of the whole target stack and between two target assemblies to prevent interference between the products from two reactions. All the Mylar foils have the same thickness, 10.5 mg/cm².

The target stack was mounted in the front of a Faraday cup in an evacuated chamber. A voltage of negative 100 V was imposed on a biasing ring of the Faraday cup to suppress the escape of the electrons. ~47 MeV/A ^{12}C ions delivered from the cyclotron passed through the Nb target assembly first, then the Cu target assembly. After penetrating through the Mylar foils and Nb target the energy of ^{12}C ions at the center of the Cu target was 527 MeV or 43.9 MeV/A [8]. The irradiation lasted for 39 hours and the beam intensity was recorded at periodic intervals by a current integrator. The integrated flux was 746 μC or 7.8×10^{14} ^{12}C ions, with typical intensities of 5-10 nA.

Following irradiation, the forward and backward catcher foils and the target were assayed with calibrated HPGe γ -ray spectrometers. The measurements of γ radioactivity were begun at 33 minutes after the end of irradiation and were taken for two months, the longest acquisition period being 14 hours. According to the intensity of γ -activity, the distance between the samples and the detector surface was varied in the range of 20-4 cm in order to reduce the count loss owing to the dead time and the coincidence of γ -rays in cascade.

The γ -ray spectra recorded on 4096 channels were analyzed with the code SAMPO [9]. The decay curves were analyzed with the code TAU88 run on graphic terminal Tektronix-4014. Radio-nuclidic assignments and calculation of the yields were described elsewhere [10]. Nuclear data used for the yield calculation were quoted from Ref. [11]. The production cross sections of the nuclides were obtained by summing up the yields from the catcher foils and the target.

Table 1
Cross sections for the production of radionuclides
in 44MeV/A $^{12}\text{C} + \text{Cu}$ reaction

Nuclide	Cross section (mb)	Nuclide	Cross section (mb)	Nuclide	Cross section (mb)
^{22}Na	3.24 ± 0.45	^{48}Sc	1.44 ± 0.13	^{57}Ni	3.08 ± 0.18
^{24}Na	2.74 ± 0.36	^{48}V	43.1 ± 3.0	^{58}Co	92 ± 12
^{28}Mg	0.21 ± 0.02	^{48}Cr	1.02 ± 0.08	$^{58}\text{Co}^m$	88 ± 11
^{41}Ar	0.94 ± 0.12	^{49}Cr	10.4 ± 2.6	^{59}Fe	3.55 ± 0.26
^{42}K	6.91 ± 0.70	^{52}Mn	40.6 ± 2.5	^{60}Co	25.7 ± 2.4
^{43}K	2.07 ± 0.15	$^{52}\text{Mn}^m$	6.6 ± 4.3	^{60}Cu	14.6 ± 1.6
^{43}Sc	7.6 ± 2.8	^{52}Fe	0.54 ± 0.05	^{61}Cu	49.8 ± 3.8
^{44}Sc	8.5 ± 1.0	^{54}Mn	79.1 ± 7.8	^{62}Zn	5.79 ± 0.45
$^{44}\text{Sc}^m$	18.4 ± 1.4	^{55}Co	5.32 ± 0.42	^{63}Zn	18.9 ± 2.0
^{46}Sc	20.2 ± 1.7	^{56}Mn	8.12 ± 0.54	^{65}Zn	17.3 ± 1.9
^{47}Ca	0.12 ± 0.02	^{56}Co	32.0 ± 2.1	^{67}Ga	0.50 ± 0.11
^{47}Sc	7.48 ± 0.71	^{57}Co	110.7 ± 8.5		

Table 2
Recoil properties of residues from 44MeV/A $^{12}\text{C} + \text{Cu}$ reaction

Nuclide	FW (mg/cm ²)	F/B	$\nu_{//} / \nu_{CN}$	Nuclide	FW (mg/cm ²)	F/B	$\nu_{//} / \nu_{CN}$
^{22}Na	5.8 ± 1.8	1.61 ± 0.51		^{52}Mn	2.01 ± 0.12	206 ± 21	0.47 ± 0.05
^{24}Na	4.41 ± 0.64	6.7 ± 1.6		$^{52}\text{Mn}^m$	2.0 ± 1.5		0.45 ± 0.34
^{28}Mg	4.56 ± 0.69			^{52}Fe	1.94 ± 0.30		0.47 ± 0.07
^{42}K	2.32 ± 0.35		0.53 ± 0.08	^{54}Mn	1.80 ± 0.28	94 ± 43	0.41 ± 0.06
^{43}K	2.43 ± 0.22	54.9 ± 9.5	0.54 ± 0.05	^{53}Co	1.59 ± 0.17	56 ± 45	0.38 ± 0.04
^{43}Sc	2.19 ± 0.86	103 ± 48	0.53 ± 0.20	^{56}Mn	1.46 ± 0.16	55 ± 46	0.34 ± 0.04
^{44}Sc	2.18 ± 0.32	241 ± 187	0.53 ± 0.07	^{56}Co	1.54 ± 0.10	85 ± 56	0.37 ± 0.04
$^{44}\text{Sc}^m$	2.34 ± 0.18	108 ± 11	0.55 ± 0.05	^{57}Co	1.36 ± 0.15		0.33 ± 0.04
^{46}Sc	2.17 ± 0.23	60 ± 13	0.50 ± 0.05	^{57}Ni	1.40 ± 0.14		0.34 ± 0.03
^{47}Sc	2.19 ± 0.32	61 ± 11	0.49 ± 0.07	^{58}Co	1.04 ± 0.16	29 ± 5	0.30 ± 0.04
^{48}Sc	2.00 ± 0.21	88.9 ± 5.5	0.44 ± 0.05	^{59}Fe	0.96 ± 0.17		0.25 ± 0.04
^{48}V	2.13 ± 0.15	150 ± 55	0.50 ± 0.05	^{60}Co	0.65 ± 0.06		0.20 ± 0.02
^{48}Cr	2.30 ± 0.24		0.54 ± 0.05	^{60}Co	0.74 ± 0.16		0.22 ± 0.05
^{49}Cr	2.01 ± 0.87		0.48 ± 0.20	^{61}Cu	0.65 ± 0.07		0.20 ± 0.02
^{51}Cr	2.07 ± 0.32		0.48 ± 0.07	^{62}Zn	0.72 ± 0.11		0.22 ± 0.03

3. RESULTS

3.1 Cross Section

The production cross sections were determined for 35 nuclides from ^{22}Na to ^{67}Ga in this work (see Table 1). The uncertainties are the standard deviations including the errors in analysis of γ -spectra and in resolution of the decay curves by the least square method and a 5% error in detector efficiencies. While the uncertainty in the thickness of the target is negligible, the beam measurement error is not included. With the exception of ^7Be and ^{24}Na produced directly from the interaction of

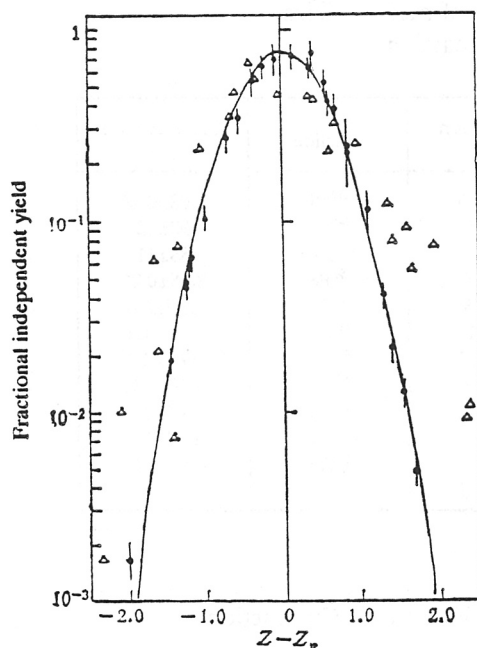


Fig. 1
The charge distribution for 44
MeV/A $^{12}\text{C} + \text{Cu}$ reaction.
♦ - experimental measurement;
Δ - theoretical calculations.

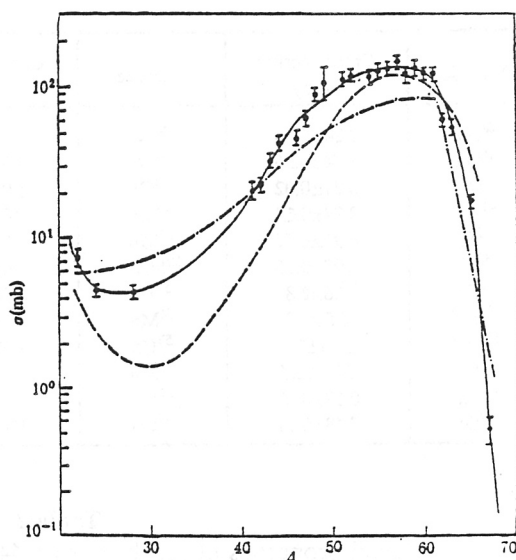


Fig. 2
The mass distributions for $^{12}\text{C} + \text{Cu}$ reactions.
— 44 MeV/A (This work); - - 35 MeV/A [4];
- · - 86 MeV/A [1].

Mylar foil with ^{12}C ions, none of the other activities were found in the Mylar foils serving as activation blanks, indicating that the Mylar foils used in this experiment were thick enough to stop all the radioactivities recoiled from the Nb target. The production cross section for ^{24}Na given in Table 1 has been corrected for the radioactivity of direct production in the Mylar.

3.2 Charge Distribution

Although a large number of cross sections of nuclides have been measured in this work, the data represent only a fraction of the total reaction cross section. In order to obtain the mass yield distribution, it is necessary to estimate the cross sections of the unmeasured nuclides by means of the charge distribution function. Accordingly, one assumes that the independent yields $\sigma(Z, A)$ of the isobaric nuclides can be expressed by a Gaussian charge distribution function:

$$\sigma(Z, A) = \sigma(A) \times \frac{1}{\sqrt{2\pi\sigma_z^2}} \exp\left\{-\frac{[Z - Z_p(A)]^2}{2\sigma_z^2}\right\}, \quad (1)$$

where $\sigma(A)$ is the mass yield, i.e., the sum of the independent yields of the various isobaric nuclides with a given mass number; σ_z is a width parameter of the charge distribution; and $Z_p(A)$ is the most probable charge for the given mass number and can be calculated by an expression:

$$Z_p(A) = K_0 + K_1 A + K_2 A^2 \quad (2)$$

where K_0 , K_1 and K_2 are constants; A is mass number. In this work the yields were determined for three nuclides, ^{48}Sc , ^{48}V and ^{48}Cr , at the mass chain of $A = 48$. Corrected for β^+ -decay feeding from the precursors, one may get the solutions of the equation (1): $\sigma_z = 0.529$ and $Z_p = 22.47$. These values are very close to those employed by Lund and Cho *et al.* for 86 MeV/ A and 35 MeV/ A $^{12}\text{C} + \text{Cu}$ reactions [1,4], showing that the parameters of the charge distribution are insensitive to the variation of the incident energy in the energy region under study. Consequently we took K_1 and K_2 in equation (2) to be 0.479 and -2.15×10^{-4} respectively [4]. With fixed $\sigma_z = 0.529$, the fractional independent yields $\sigma(Z, A)/\sigma(A)$ corrected for β -decay feeding from the precursors were used to fit the Gaussian charge distribution function of equation (1) by adjusting the K_0 value for each mass region. Only for the products close to the target ($59 < A < 67$), the width parameter σ_z of the charge distribution was taken as 0.58 in order to get a better fit.

Fig. 1 shows the Gaussian charge distribution curve with the width parameter of $\sigma_z = 0.529$. For the products with mass number $A < 58$, the experimental independent yield corrected for β -decay feeding are in good agreement with the Gaussian curve. The mass yield distribution calculated on the basis of the assumption on the charge distribution is shown in Fig. 2. Unlike some other works [4,5], no assumptions about the form of the mass distribution curve are needed in this work.

3.3 Recoil Properties

In terms of the activity in the forward and backward catcher foils, one may calculate F and B values which represent the fractions of the total activity of a given nuclide collected in the forward and backward catches, respectively. These two values are a combined measure associated with the recoil angular distribution and recoil range. In the thick target-thick catcher foil experiment a more interesting quantity is the average forward range, FW , and the ratio of forward-to-backward emission, F/B where W is the target thickness. The results are listed in Table 2. The uncertainties were determined on the basis of the propagation of the errors. In addition to direct production of ^{24}Na in the Mylar, it was found that the activity of ^{24}Na in the downstream was significantly larger than that in the upstream foil, indicating a large enough forward range of ^{24}Na produced in Mylar. As a result a significant fraction of ^{24}Na activity was transferred into the adjacent downstream foil. The correction can be made for ^{24}Na recoil because the ^{24}Na activity of three blank Mylar foils with different geometric arrangement was measured in this experiment.

In the interaction of Cu with 44 MeV/ A ^{12}C ions the mean forward ranges in the target decrease with increasing mass number of the target residues. It is particularly noticeable that the lightest products, ^{22}Na , ^{24}Na and ^{28}Mg have very large recoil ranges. It can also be seen from Table 2 that with the exception of ^{22}Na , ^{24}Na , the F/B ratios are very large, typically around 100. The behaviour of the recoils indicate that the target residues are produced with substantial momentum transfer.

4. DISCUSSION

4.1 Mass Distribution

It can be seen in Fig. 2 that the mass distribution shows a broad peak slightly below the target mass, with the peak position being at $A \sim 57$. With decreasing mass number, the yields decrease to a minimum at $A \sim 30$; and then increase inversely with mass number. The unique trans-target

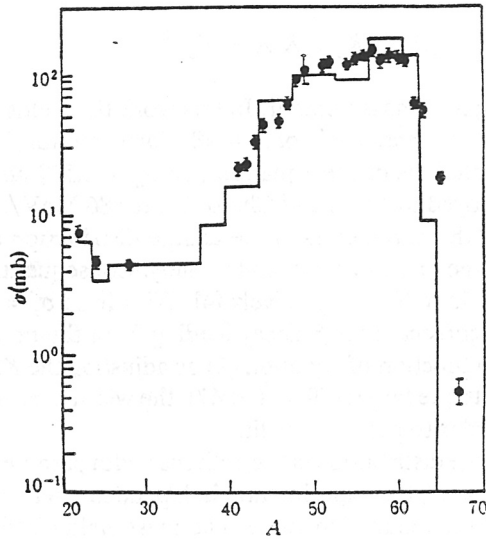


Fig. 3

Comparison of the experimental mass distribution with that calculated by the modified statistical model.

product observed in the interaction of copper with 35 MeV/A and 86 MeV/A ^{12}C ions was ^{65}Zn . In addition to ^{65}Zn , in this work we also observed ^{67}Ga , the production cross section being only 0.5 mb.

The mass distribution has a similar overall shape to those of the interactions of copper with 35 MeV/A and 86 MeV/A ^{12}C ions (see Fig. 2). However some differences may still be noted. With increasing incident energy, the peaks of the mass distributions broaden, the logarithmic slopes of decreasing yields with the mass number drop off and the relative yields of the nuclides with the lightest mass number rise. The average mass number obtained in this work, 53.4 u, is between 55.2 u and 51.1 u obtained from 35 MeV/A and 86 MeV/A, respectively. This result suggests that in the energy region studied in this work higher excitation energies are available at the higher bombarding energy leading to larger mass losses.

Cumming *et al.* [12] have found that the logarithmic slope of the mass yield curves in the exponential region decreases with increasing bombarding energy and was an approximate measure of the mean excitation energy transferred to the composite system in the initial interaction. The mass distribution measured in this work does not vary exponentially over the given mass region. Nevertheless, in order to compare with the other data, as done by Cho *et al.* [4], we have fitted the data in the region between $A = 33$ and 57 with an exponential. Resultant slope is 12.5% per mass number and is between 19% and 9% for 35 MeV/A and 86 MeV/A $^{12}\text{C} + \text{Cu}$ reaction. This value also agrees with the Cumming systematics.

By integrating the mass distribution in Fig. 2 over the $A = 28$ -65 mass range we obtain the total reaction cross section of 2.33 ± 0.33 b. The yields at $A < 28$ are not taken into account. It is sure that these products were formed from a binary or even multi-fragmentation process. Kox *et al.* have proposed a expression for parametrization of the total reaction cross section [13]. Saint-Laurent *et al.* determined the total reaction cross section values in a wide span of projectile-target systems by means of the $4\pi - \gamma$ method and found that the experimental results could be well described by the

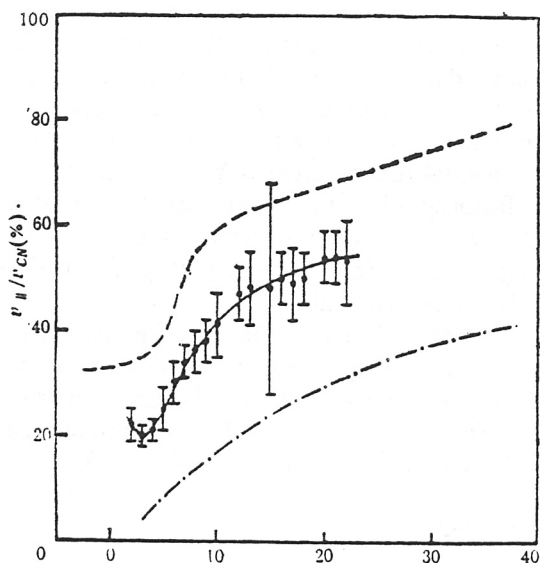


Fig. 4
Variation of the fractional LMT with mass loss.
— 44 MeV/A (This work); — 35 MeV/A [4];
- · - · - 86 MeV/A [3].

formula developed by Kox *et al.* [14]. Using the same parameter, the total reaction cross section was calculated to be 2.20 b, which is in remarkably good agreement with the result of this work.

4.2 Comparison With Statistical Model Calculation

The statistical model describing the fragmentation process in a high energy heavy ion reaction was, after modification, applied to the intermediate energy heavy ion reaction and successfully reproduced the mass distribution of the target residues from the 35 MeV/A $^{12}\text{C} + \text{Cu}$ reaction [7]. In this work the modified statistical model and corresponding Monte Carlo technique were used again to calculate the mass and charge distributions for the 44 MeV/A $^{12}\text{C} + \text{Cu}$ reaction in order to observe if the experimental results agree with the theoretical prediction at a different incident energy. The theoretical parameters $R_{TO} = 1.90$ fm, $C_p = 0.73$ were used in the calculation (where R_{TO} and C_p are the radius parameters characterizing the volume of the freeze-out state and a fractional factor of effective excitation-energy, respectively). The comparison between experimental data and theoretical predictions is shown in Fig. 1 and Fig. 3.

As shown in Fig. 3 the theoretical calculations for the mass distribution of the target fragments agree quite well with the experimental data. Some features, e.g. the peak position, the slope at mass numbers of $A \sim 40$ and the upturn of the mass yields at $A < 30$ have been reproduced by the theoretical calculations. A large discrepancy, however, is present in the heavy mass region ($A > 63$). The residues in this region were formed mainly from a direct interaction between the projectile and the target, e.g. transfer reaction and inelastic scattering, which we did not attempt to take into account in the theoretical model. Therefore the discrepancy between the theory and the experiment is understandable. Around the target mass region, e.g. $56 < A < 60$, however, the agreement between the theoretical calculations and the experimental data is in contradiction, to some extent,

with the measurement of linear momentum transfer, which will be mentioned later. From the information of the linear momentum transfer we know that the products at this mass region resulted from the peripheral collision which did not lead to the formation of a composite system and was not taken into account by the theoretical calculation. Therefore the theoretical calculation seems to overestimate the yields of the products at this mass region. As a whole, however, the theoretical calculation reproduces the experimental results tolerably well. The theoretical calculations of the charge distribution agree satisfactorily with the measurements. Although two wings of the theoretically calculated charge distribution are wider than those of the experimental data, full-widths at half-maximum are in good agreement. Moreover, the peak position of the calculated charge distribution shifts slightly towards neutron-rich side.

The agreement between the theoretical and the experimental results indicate that the disassembly of hot nuclei might be depicted by a unified statistical model no matter whether the energy of the collision in which the hot nuclei were created, is high or intermediate. Moreover the agreement also suggests that multifragmentation is one of the important reaction mechanisms for the interaction of Copper with 44 MeV/A ^{12}C ions studied in this work.

4.3 Longitudinal Momentum Transfer

Longitudinal momentum transfer (LMT) measurements in a heavy ion reaction can provide the information about how the reaction mechanism evolves from complete fusion to incomplete fusion or even to fragmentation when the incident energy of the projectile increases and some features of the excitation energy are deposited in the composite system.

In the radiochemical thick target-thick catcher foil measurement LMT are extracted from the calculation of $2W(F + B)$ and F/B values on the basis of the two-step model [16]. This method has been used extensively in the study of high energy nuclear reactions. In the intermediate energy region involved in this work, as mentioned above, the momentum transfer is substantial and the recoil range is proportional to recoil velocity in this reaction. Consequently, due to particle evaporation, the velocity V imparted to residue is negligible in the second step, i.e. the deexcitation step of the reaction. Recoil velocity of the residue depends mainly on the longitudinal velocity $v_{||}$ imparted to the composite system by the projectile in the initial interaction. As done by Cho *et al.* [7], on the basis of the method proposed by Winsberg and Alexander [17], the velocity corresponding to the mean forward range of the nuclide in the target, FW , is just $v_{||}$. Furthermore the effect of the angular distribution on the calculation of $v_{||}$ was also neglected. The correction factor which would decrease the transferred momentum was estimated to be less than 15% [18]. The range-energy tables of Northcliffe and Schilling were used in performing these calculations [19]. The $v_{||}/v_{CN}$ values characterizing longitudinal momentum transfer are listed in Table 2, and $v_{CN} = 1.487 (\text{MeV}/u)^{1/2}$ is the recoil velocity of the putative compound nucleus. The $v_{||}/v_{CN}$ values for each products are plotted versus a mass loss $\Delta A (= A_T - A_P, A_T$ and A_P are the mass numbers of the target and products respectively) in Fig. 4. As seen from Fig. 4, the fractional longitudinal momentum transfer increases with the mass loss, ranging from $\sim 20\%$ for products close to the target to $\sim 54\%$ for the lighter products. The average value of the fractional LMT for the whole reaction (i.e. integrated over all impact parameters) obtained by weighing the experimental values of the mass yield distribution is 0.38 ± 0.05 , corresponding to an LMT of $1.3 \pm 0.2 \text{ GeV}/c$. The Fig. 4 also shows the similar measurements for 35 MeV/A and 86 MeV/A $^{12}\text{C} + \text{Cu}$ reactions [3,4]. The curves of $v_{||}/v_{CN}$ versus ΔA are of similar shape. It is apparent that the fractional momentum transfer decreases with increasing incident energy. This trend is consistent with the systematics of a approximately linear decrease of LMT with increase of the velocity of the projectile [20].

Examining the LMT quantitatively, however, one may find that the fractional momentum

transfer measured in this work is significantly less than the value of 0.50-0.56 predicted from *LMT* systematics [21,22]. The reason for this deviation is attributed to the fact that the *LMT* measured in this work is the average value integrated over all impact parameters including quasielastic transfer reaction with some slight momentum transfer. On the other hand, from recent studies of *LMT*, it appears that the *LMT* not only depends mainly on velocity of the projectile but is also relative to the mass number of the target and the kind of projectile. While the momentum transferred to the heavier target is larger than that transferred to the lighter target, the light projectiles such as ${}^4\text{He}$ transfer more momentum than the heavier ions do. Taking these facts into account, it is not difficult to understand the less fractional *LMT* in the ${}^{12}\text{C} + \text{Cu}$ reaction.

From the data of the longitudinal momentum transfer, one may obtain the information about the excitation energy deposited in the composite system after the initial interaction. The initial interaction between the heavy ion and target can be regarded as an incomplete fusion, with the uncaught nucleons of the projectile escaping at 0° . Following Jastzebski *et al.* [23], we assume that the evaporation of one nucleon needs to expend about 10 MeV of excitation energy. From the average mass number measured experimentally, the excitation energy of the composite system is deduced to be 150 MeV.

The excitation energy E^* of the composite system formed in the initial collision associated with the formation of the final products can be calculated by the equation [23]:

$$\frac{E^*}{E_{CN}} = 0.8 \frac{\langle \nu_{||} \rangle}{\nu_{CN}} \quad (3)$$

where E_{CN} denotes the excitation energy of the composite system formed putatively by complete fusion. Calculation indicates that the excitation energy increases with the mass loss ΔA ranging from ~ 80 MeV to 340 MeV. Considering an increase in *LMT* with increasing ΔA , we may conclude that the formation of an intermediate composite system with the higher excitation energy originates from the central collision accompanying larger *LMT*, leading to production of lighter reaction products due to the evaporation of a larger number of nucleons. On the other side, the peripheral collision results in the formation of the products close to target mass accompanying the less *LMT* and the lower excitation energy. It is very necessary for further studies of longitudinal momentum transfer to distinguish between the central collision and the peripheral collision with radiochemical techniques.

ACKNOWLEDGMENT

We appreciate the great efforts of the accelerator personnel who made our first experiments on HIRFL possible. We are grateful for the assistance of Zhang Li, Li Zongwei, Qin Zhi and Li Yunsheng in γ -ray measurement.

REFERENCES

- [1] T. Lund *et al.*, *Phys. Lett.*, **102B** (1981) 239.
- [2] T. Lund *et al.*, *Z. Phys.*, **A306** (1982) 43.
- [3] L. Kowalski, P. E. Haustein and J. B. Cumming, *Phys. Rev. Lett.*, **51** (1983) 642.
- [4] S. Y. Cho *et al.*, *Phys. Rev.*, **C36** (1987) 2349.
- [5] N. T. Porile *et al.*, *Proc. Third Inter. Conf. on Nucleus-Nucleus Collisions* (France, 1988) p65.
- [6] L. Pienkowski *et al.*, *Proc. Third Inter. Conf. on Nucleus-Nucleus Collisions* (France, 1988) p 63.

- [7] Sa Benhao, Zheng Yuming and Zhang Xiaoze, *High Energy Phys. and Nucl. Phys. (in Chinese)*, **13** (1989) 1117.
- [8] Chen Jiachao *et al.*, *High Energy Phys. and Nucl. Phys. (in Chinese)*, **15** (1991).
- [9] T. Routti and S. G. Prussion, *Nucl. Instrum. Methods*, **72** (1969) 125.
- [10] Li Wenxin and Sun Tongyu, *Atomic Energy Science and Technology*, **24** (1990) 60.
- [11] U. Reus and W. Westmeier, *At. Data Nucl. Data Tables*, **29** (1983) No.2.
- [12] J. B. Cumming *et al.*, *Phys. Rev.*, **C17** (1978) 1632.
- [13] S. Kox *et al.*, *Phys. Rev.*, **C35** (1987) 1678.
- [14] M. G. Saint-Laurent *et al.*, *Z. Phys.* **A332** (1989) 457.
- [15] Sa Benhao, Zheng Yuming and Zhang Xiaoze, "Statistical Model for the Disassembly Processes of Medium Energy Heavy-Ion Reactions" (Submitted to *Phys. Rev. C*).
- [16] L. Winsberg, *Nucl. Instrum. Methods*, **150** (1978) 465.
- [17] L. Winsberg, and J. M. Alexander, *Phys. Rev.*, **121** (1961) 518.
- [18] T. Batsch *et al.*, *Phys. Lett.*, **B189** (1987) 287.
- [19] L. C. Northcliffe and R. F. Schilling, *Nucl. Data Tables*, **A7** (1970) 233.
- [20] V. Viola *et al.*, *Phys. Rev.*, **C36** (1982) 178.
- [21] E. Tomasi *et al.*, *Proc. Second Inter. Conf. on Nucleus-Nucleus Collisions*, Vol. 1, p 60.
- [22] J. Jastrzebski *et al.*, *Phys. Lett.*, **136B** (1984) 153.
- [23] J. Jastrzebski *et al.*, *Phys. Rev.*, **C34** (1986) 60.